

**U.S. DEPARTMENT OF COMMERCE  
National Technical Information Service**

**N76-23663**

**CLASSIFYING AND MONITORING WATER QUALITY BY USE  
OF SATELLITE IMAGERY**

**J. P. SCHERZ, ET AL**

**BENDIX AEROSPACE SYSTEMS DIVISION  
ANN ARBOR, MICHIGAN**

**SEPTEMBER 1975**



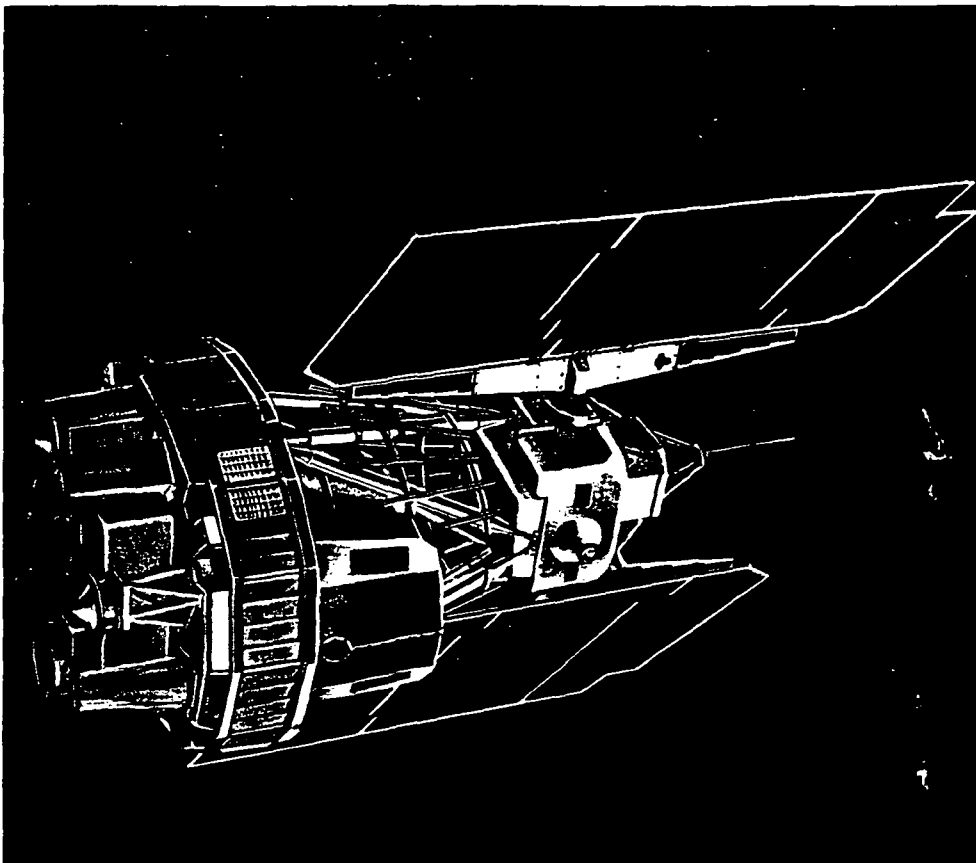
DRA

# Classifying and Monitoring Water Quality by use of Satellite Imagery

Prepared for:

International Conference  
on Environmental Sensing  
and Assessment

September 14-19, 1975  
Las Vegas, Nevada



(NASA-CF-144752) CLASSIFYING AND MONITORING  
WATER QUALITY BY USE OF SATELLITE IMAGERY  
(Bendix Corp.) 27 p HC CSCL 08H

N76-23663

Unclas  
G3/43 15117

REPRODUCED BY  
NATIONAL TECHNICAL  
INFORMATION SERVICE  
U. S. DEPARTMENT OF COMMERCE  
SPRINGFIELD, VA. 22161

Prepared by:

Bendix Aerospace Systems Division  
3621 South State Road  
Ann Arbor, Michigan 48107  
Tel (313) 665-7766

Dept. of Civil and Environmental Engineering  
University of Wisconsin  
Madison, Wisconsin 53706



**Aerospace  
Systems Division**

PRICES SUBJECT TO CHANGE

## **N O T I C E**

**THIS DOCUMENT HAS BEEN REPRODUCED FROM THE  
BEST COPY FURNISHED US BY THE SPONSORING  
AGENCY. ALTHOUGH IT IS RECOGNIZED THAT CER-  
TAIN PORTIONS ARE ILLEGIBLE, IT IS BEING RE-  
LEASED IN THE INTEREST OF MAKING AVAILABLE  
AS MUCH INFORMATION AS POSSIBLE.**

**TECHNICAL REPORT STANDARD TITLE PAGE**

1. Report No.		2. Government Accession No.		3. Recipient's Catalog No.	
4. Title and Subtitle Classifying and Monitoring Water Quality by Use of Satellite Imagery				5. Report Date September 1975	
				6. Performing Organization Code	
7. Author(s) J. P. Scherz, D. R. Crane & R. H. Rogers				8. Performing Organization Report No. BSR 4197	
9. Performing Organization Name and Address Bendix Aerospace Systems Division 3621 South State Road Ann Arbor, Michigan 48107				10. Work Unit No.	
				11. Contract or Grant No. NAS5-20942	
12. Sponsoring Agency Name and Address Goddard Space Flight Center Greenbelt, Md. 20771				13. Type of Report and Period Covered  Special Report	
				14. Sponsoring Agency Code	
15. Supplementary Notes Dr. Rogers is with Bendix, Dr. Scherz and Mr. Crane are with the University of Wisconsin. The paper is being presented at the International Conference on Environmental Sensing & Assessment, Sept. 14-19, 1975, Las Vegas, Nevada					
16. Abstract  Of particular importance is the development of a technique in which LANDSAT measurements from very clear lakes are subtracted from measurements from other lakes in order to remove atmospheric and surface noise effects to obtain a residual signal dependent only on the material suspended in the water. This residual signal is used by the Bendix Multispectral Data Analysis System as a basis for producing color categorized imagery showing lakes by type and concentration of suspended material. Several hundred lakes in the Madison and Spooner, Wisconsin area were categorized for tannin or non-tannin waters and for the degree of algae, silt, weeds, and bottom effects.					
17. Key Words (Selected by Author(s)) Water Quality, Computer Processing, Lake Eutrophication, LANDSAT, Multispectral Data				18. Distribution Statement	
19. Security Classif. (of this report)		20. Security Classif. (of this page)		21. No. of Pages	
				22. Price*	

**CLASSIFYING AND MONITORING WATER QUALITY  
BY THE USE OF SATELLITE IMAGERY**

---

**James P. Scherz and Douglas R. Crane  
Dept. of Civil and Environmental Engineering  
University of Wisconsin  
Madison, Wisconsin 53706**

**Robert H. Rogers  
Bendix Aerospace Systems Division  
3621 South State Road  
Ann Arbor, Michigan 48107**

**September 1975  
Special Report**

**Prepared for:**

**GODDARD SPACE FLIGHT CENTER  
Greenbelt, Maryland 20771**

CLASSIFYING AND MONITORING WATER QUALITY  
BY USE OF SATELLITE IMAGERY

James P. Scherz and Douglas R. Crane  
University of Wisconsin  
Madison, Wisconsin 53706

Robert H. Rogers  
Bendix Aerospace Systems Division  
Ann Arbor, Michigan 48107

BIOGRAPHICAL SKETCHES

James P. Scherz is an Associate Professor in the Department of Civil and Environmental Engineering at the University of Wisconsin where he teaches surveying, photogrammetry, remote sensing and related subjects. His primary research work is with remote sensing of water quality.

Douglas R. Crane is completing a M.S. degree in Civil and Environmental Engineering at the University of Wisconsin. His graduate research work has been on remote sensing of water quality.

Robert H. Rogers is a senior staff engineer at Bendix Aerospace Systems Division where he is a principal investigator for NASA/ERTS and co-investigator for NASA/Skylab programs.

ABSTRACT

By use of distilled water samples in the laboratory, and very clear lakes in the field, a technique has been developed where the atmosphere and surface noise effects on LANDSAT signals of water bodies can be removed. The residual signal is dependent only on the material in the water. The general type and concentration of the material can be determined from LANDSAT tapes. When this material in the water is living algae or weeds, its concentration is related to the enrichment or eutrophication of the lake. The algae and weed biomass is at a maximum in late August which is therefore the optimum time to categorize lakes.

For this project, the Wisconsin Department of Natural Resources helped provide water samples, and the University of Wisconsin under NASA support helped provide laboratory and computer analysis and aerial observation of the lakes. The Bendix Multispectral Data Analysis System (M-DAS) provided a Color Categorized Image of several hundred lakes. These lakes were categorized for tannin or non-tannin waters and for the degrees of algae, silt, weeds, and bottom effects present. The initial categorization is being field checked in late August 1975.

## INTRODUCTION

When LANDSAT images are used for mapping land targets essentially two factors are involved: (1) How the sun and skylight interact with the target to form a reflected signal, and (2) how the atmosphere effects this signal before it reaches the sensor. Land targets are considered as diffuse reflectors and Lambert's Law for diffused reflection can be used in the analysis.

When LANDSAT images are used for mapping or monitoring water quality the process becomes more complex. Sunlight and skylight interact with water surface, the particles in the water volume, and in some cases with the bottom. The signal from the water surface must be treated as primarily specular reflection but there is a small surface diffused reflection component caused by dust, foam and other contaminants on the water surface. The surface specular component varies greatly depending on the skylight condition and is essentially independent of the material in the water volume (1). The signal from the water volume can be treated as diffused reflection from the suspended particles in the water. The signal from the bottom is troublesome noise which follows the laws of diffused reflection. All of these signals combine to form the total signal from the lake or other water body. This total signal is modified by the atmosphere prior to its reaching the satellite sensor.

The most important component of the signal from the water is that caused by the material in the water volume. This is called volume reflectance or backscatter and is herein denoted by  $\rho_v$ . There is a different  $\rho_v$  for each color (wavelength). The volume reflectance for a water is primarily caused by light being diffusely reflected from suspended particles in the water between the water surface and the depth where the energy is extinguished. Pure or distilled water is assumed to contain no suspended material; therefore the volume reflectance of the suspended particles in distilled water is essentially zero. However, even in the laboratory there will be some diffuse backscatter from distilled water caused by the water molecules, dust, foam, or other impurities on the water surface. Let the laboratory diffused reflectance from impurities on the water surface be indicated by  $\rho_{SL}$ . There is a different  $\rho_{SL}$  for each color or wavelength of energy.

As material is added to a pure water sample the only factor that will be significantly altered will be the volume reflectance,  $\rho_v$ . The dust, foam and other impurities are likely to remain unchanged so the  $\rho_{SL}$  should not change. In some cases oil slicks can alter this  $\rho_{SL}$  but in all other cases it is considered unchanging. It is  $\rho_v$ , volume reflectance, which changes as material is added to the water. The type and amount of material added to pure water is what alters the water quality. Each type of material such as red clay, green taconite mine tailings, blue-green algae, etc. reflect differently at different wavelengths. These different materials have unique spectral reflectance signatures which are indicated by the  $\rho_v$  at different wavelengths. The LANDSAT Satellite has four different sensor bands so the type of material in water should be detectable from the four bands of LANDSAT.

For a particular size and shape of particle, as more material is added to the water there will be more particles to backscatter the light. The volume reflectance,  $\rho_v$ , will increase as will the total signal sensed by the



Satellite. Therefore, for a particular type of material, its concentration should be related to the LANDSAT signal strength.

It should be possible to determine both the type of material and its general concentration from LANDSAT images. To do so one must manipulate the total signal from LANDSAT so that only the volume reflectance,  $\rho_v$ , is left as a residual. Only  $\rho_v$  relates to the types and concentrations of materials in water. Surface effects, bottom effects, and atmospheric effects are all noise sources which must be removed. In order to remove these effects the volume reflectance,  $\rho_v$ , of distilled water or a very clear lake approaching distilled water must be determined in the laboratory or by use of the Bendix Radiant Power Measuring Instrument (RPMI) (2). Laboratory values are more precise than field values because in the field one must contend with indirect skylight and wave action which can be eliminated in the laboratory. On the LANDSAT image a clear lake which approaches distilled water must be used for calibration. With the LANDSAT signal from this lake and the known volume reflectance for its clear water it is possible to eliminate the surface and atmospheric effects and have residual signals which are indicative only of the type and concentration of the material in other lakes.

#### MADISON AREA LAKES

Figure 1 shows two LANDSAT images of lakes near Madison, Wisconsin. The upper image is taken in early spring shortly after the ice had thawed; there was essentially no algae growth in any of the lakes. All lakes appear essentially the same brightness on the LANDSAT image.

The lower image shows the same area in late August when algae and weed growth are at a maximum. Those lakes which have an abundance of nutrients (eutrophic lakes) have heavy algae growths. Skylight and sunlight interact with this suspended algae and is backscattered to the satellite. The denser the algae growth, the more the backscatter and the brighter it appears on the LANDSAT image. A clear (oligotrophic lake) such as Devil's Lake does not have enough nutrients present to sustain significant algae growth and it has approximately the same strength of backscattered signal in August as in early spring. The highly eutrophic lakes such as Lake Kegonsa have backscattered signals so high in August that they are virtually indistinguishable from the green fields in Figure 1.

The backscatter from a lake can be sensed in the four bands of the LANDSAT satellite. The long-established water quality parameter used to indicate backscatter is turbidity. Turbidity is an average value determined across the visible spectrum and its units are expressed as FTU's. Figure 2 shows the strength of the backscatter signal from Madison area lakes as sensed from the LANDSAT satellite on two different days in late summer. These signals are plotted against turbidity. It is obvious from Figure 2 that for a particular day there is a good correlation between the LANDSAT signal and turbidity and eutrophic classification. However, for a different day the height of this correlation curve shifts. This shift is caused by different atmospheric parameters from day to day. If one can determine the exact location of the curve for a particular day it can be used to map turbidity if there are no tannin lakes present nor lakes where bottom effects are significant.

For tannin lakes, the tannic acid in the water creates a dark brown color

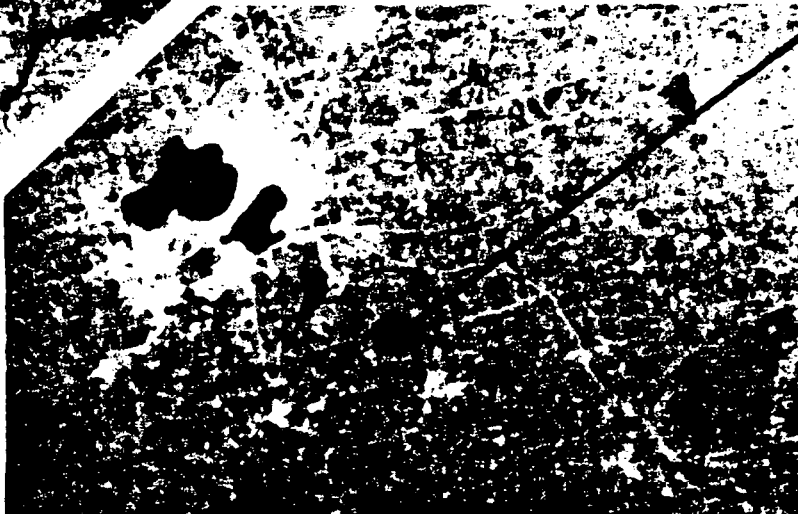
APRIL



Devil's Lake (Clear and Oligotrophic)

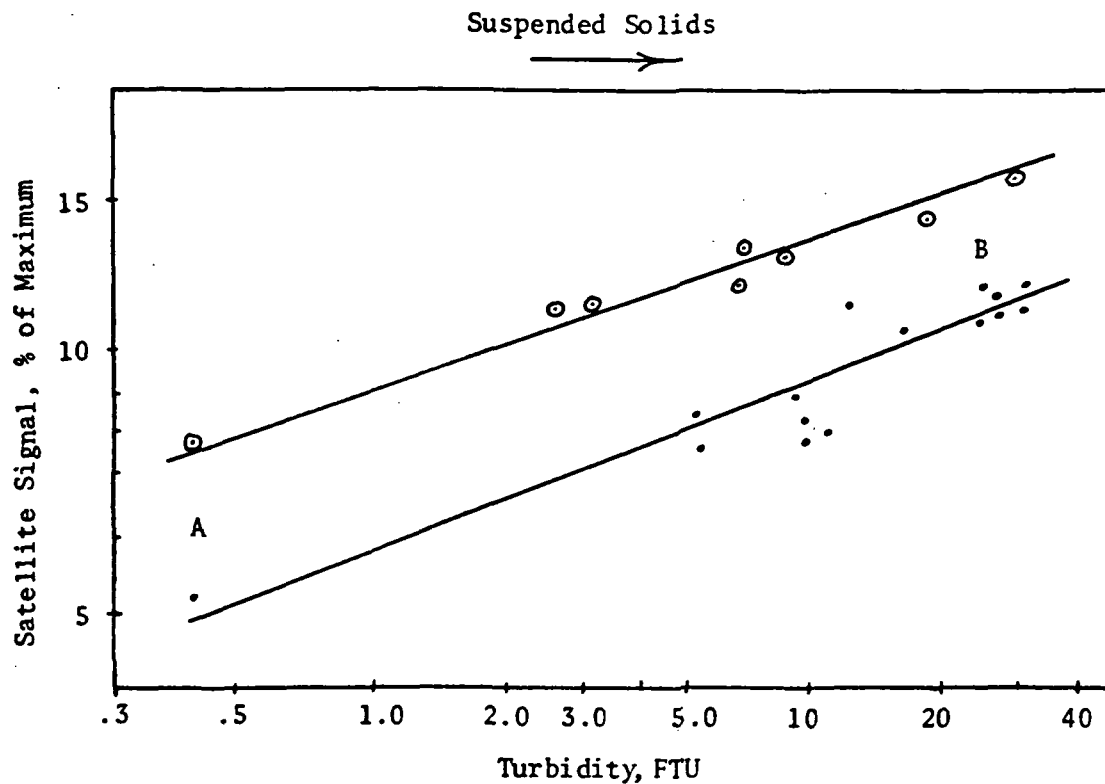


Lake Kegonsa (Algal and Eutrophic)



LATE AUGUST

FIGURE 1 ERTS (LANDSAT) Images of Lakes near Madison, Wisc. in early Spring when Algae and Lake Weed Growth is a Minimum and in Late August when it is Maximum. Band 5 (Red)



• = 28 August 1972

⊙ = 5 August 1973

A = Devil's Lake (clear, oligotrophic lake)

B = Lake Kegonsa (algae filled and eutrophic)

Figure 2. Strength of backscatter signal received by Band 5 of ERTS (LANDSAT), Madison Area Lakes. Note shift in height of curve for different days due to atmospheric change.

which absorbs energy. On the curve of Figure 2 such a lake would lie below the curve for the other lakes. For a lake with strong bottom effects the signal from say a sand bottom would create a point which lies far above the curve for the other lakes. In order to handle tannin and sand bottom lakes the spectral signatures must be analyzed first so the lakes can be put into classes of essentially tannin lakes, non-tannin lakes and bottom lakes. Within a class the curves, such as those in Figure 2, can be used to categorize the lakes as to turbidity and possible eutrophic classification. The lakes in Figure 2 are essentially non-tannin lakes with various amounts of algae present and no bottom effects.

In Figure 2 the shift of the signal-turbidity curve is considerable. There is no universal curve for all days. On the other hand, the laboratory curve of backscatter versus turbidity is essentially universal for all days. Figure 3 shows such a curve which combines laboratory red-light backscatter values for 127 samples analyzed over three years at the University of Wisconsin. Values for tannin lakes tend to fall slightly below the average curve and form a curve of their own, but generally speaking the laboratory backscatter versus turbidity curve is a universal curve. The laboratory backscatter in Figure 3 is indicated on the y axis by the apparent laboratory reflectance,  $AP$ , where

$$AP = \frac{\rho_V + \rho_{SL}}{\rho_{PL}}$$

and  $\rho_{PL}$  is the diffuse reflectance of the standard laboratory reflection panel. The calculated value of  $\rho_{PL}$  for .65 microns was 39%. The average approximate value of  $\rho_{SL}$  can be considered about 0.020%. With these values one can, with any  $\rho_V$ , obtain the corresponding expected value of turbidity. Once turbidity is known it is then possible to map other water quality parameters which might correlate to turbidity for that particular type of water.

The correlation of other water quality parameters such as suspended solids to turbidity is not universal but varies for different waters. It is possible to have a few large particles of dark material which have a certain weight which scatter back considerably less energy than say a large number of exceedingly fine white particles of the same total weight. For the same sized and shaped particles of a certain material there is a correlation between weight of suspended material and turbidity, but one must point out that this correlation will not necessarily hold for another material in a different type water.

When the material causing the turbidity or backscatter is say algae then there may also be a correlation between backscatter (satellite signal strength) and chlorophyll. But try the same correlation on an inorganic red clay and the backscatter-chlorophyll correlation breaks down. If the suspended material causing turbidity is municipal or industrial sewage which upon decay uses oxygen then for this situation there may be a correlation between backscatter (remote sensing signal strength) and Biological Oxygen Demand (BOD), or the dissolved oxygen which is not yet used up (3). However, try the same correlation on inorganic red clay in water and the correlation breaks down. For all waters however, the correlation of backscatter (volume reflectance,  $\rho_V$ ) and turbidity holds as shown in Figure 3. For Red Energy (.65 microns) this correlation is:  $T = 5.21(AP)^{2.00}$

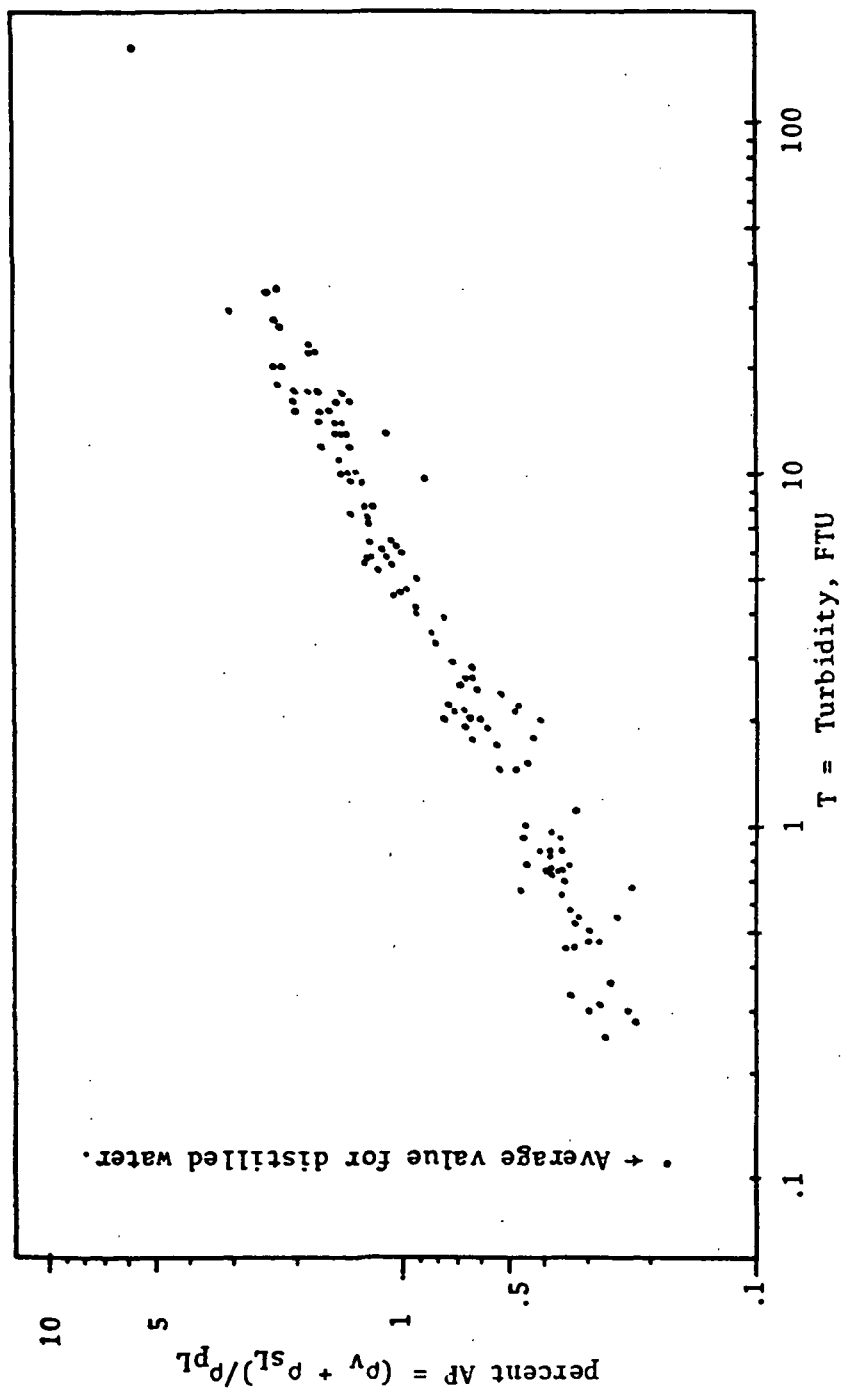


Figure 3. Laboratory backscatter expressed as apparent laboratory reflectance, AP, plotted against turbidity for 127 different lake samples collected over three years. This curve is for red light (0.65 microns). The best fit equation for this data is  $T = 5.21 (AP)^{2.00}$

For this investigation, the volume reflectance values,  $\rho_v$ , for a water are obtained for different wavelengths, some of which correspond to the LANDSAT bands. The resulting spectral signature allows one to put lakes into general categories such as tannin or non-tannin waters. Then within a category a curve such as in Figure 3 can be used to categorize the lakes as to relative turbidity and the amount of suspended material such as algae which causes this turbidity.

### LABORATORY ANALYSIS

The volume reflectance,  $\rho_v$ , can be obtained by the scheme shown in Figure 4. In a darkened laboratory, a laboratory lamp provides light onto a standard  $\text{BaSO}_4$  diffuse reflection panel and onto the water sample. The water sample is in a tube .62 meters long which has a black bottom. Shorter tubes will cause overriding bottom signals which make the results confusing or meaningless as will a bottom which is too reflective (4)(5). The sides of the tube are lined with diffusely reflecting white chronoflex which returns side-scattered energy simulating adjacent water volumes in the field.

The radiance of the lamp is  $L_L$  in watts/cm<sup>2</sup> s. As viewed from the level of the panel or water sample the solid angle of the lamp is  $\psi_L$  steradians. The total irradiance that reaches the level of the panel at right angles to the rays is  $L_L \psi_L$ . The total irradiance available on the panel per unit area is

$$H_L = L_L \psi_L \cos \theta \text{ (Watts/cm}^2\text{)}$$

where  $\theta$  is the angle between the lamp and the vertical as shown in Figure 4. The indirect illumination from the ceiling  $L_c$  (watts/cm<sup>2</sup> s) is zero in the perfect laboratory setup.

Lambert's Law states that  $P$ , the diffuse radiance returning into space from the panel, is

$$P = \frac{H_L}{\pi} \rho_{PL} \quad \text{equation 1}$$

where  $\rho_{PL}$  is the diffuse reflectance of the panel.

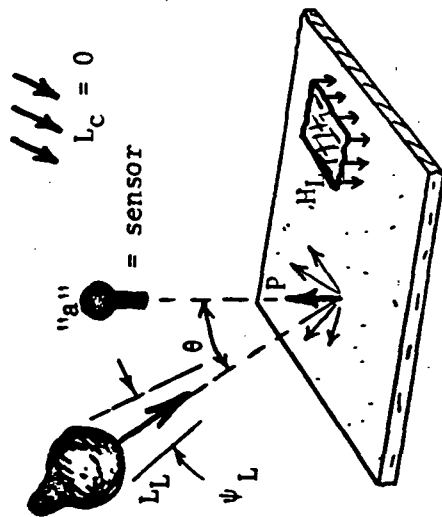
Since the dust, foam and other impurities on the water surface also behave as diffuse reflectors their signal,  $S_L$ , also follows Lambert's Law

$$S_L = \frac{H_L \rho_{SL}}{\pi}$$

where  $\rho_{SL}$  is the diffuse reflectance of the impurities on the water surface in the laboratory. The suspended particles in the water volume are also diffuse reflectors and cause the radiance from the water volume  $V$ .

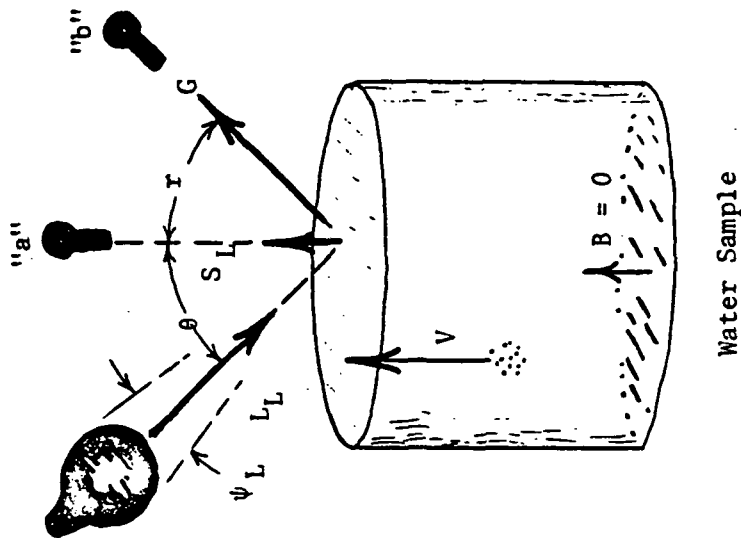
$$V = \frac{\rho_v H_L}{\pi}$$

where,  $\rho_v$  = the diffuse reflectance of the particles in the water volume. This  $\rho_v$  is the all-important factor which is indicative of water quality.



Standard Diffuse Reflection Panel

$L_L$  = Radiance of Laboratory Lamp, Watt/cm<sup>2</sup> s  
 $H_L$  = Irradiance on Horizontal Panel caused by Lamp, Watt/cm<sup>2</sup>



Water Sample

P, S, V, and B are Radiance values (Watt/cm<sup>2</sup> s) caused by Diffuse Reflection  
 G is glitter Radiance (Watt/cm<sup>2</sup> s) caused by specular reflection

Figure 4. Direct Energy Relationships in the Laboratory

The signal G does not follow the laws of diffuse reflection. When  $\theta = r$ , as in Figure 4, the signal G is specular reflection of the lamp's radiance from the air-water interface.

$$G = \phi L_L \text{ (Watts/cm}^2\text{s)}$$

where  $\phi$  = the surface specular reflection of a water-air interface.

$$\phi = \frac{(n_w - n_a)^2}{(n_w + n_a)^2} \quad \text{where}$$

$n_w$  = index of refraction of water = 1.333, and  
 $n_a$  = index of refraction of air = 1.000.

$$\phi = \frac{(1.333 - 1.000)^2}{(1.333 + 1.000)^2} = 0.020$$

This value holds fairly well out to angles of  $\theta$  and  $r$  of about 40 degrees of the vertical. Most remote sensing operations fall within this range.

The total signal from the water as seen by the sensor is w

$$W = V + S_L$$

$$W = \frac{\rho_V H_L}{\pi} + \frac{\rho_{SL} H_L}{\pi}$$

$$W = (\rho_V + \rho_{SL}) \frac{H_L}{\pi} \quad \text{equation 2}$$

The ratio of this signal W to the signal from the panel is called apparent laboratory reflectance AP.

$$AP = \frac{W}{P} = \frac{\frac{H_L}{\pi} (\rho_V + \rho_{SL})}{\frac{H_L}{\pi} (\rho_{PL})} = \frac{\rho_V + \rho_{SL}}{\rho_{PL}} \quad \text{equation 3}$$

The  $\rho_{PL}$  reflectance for  $\text{BaSO}_4$ , for 0.65 microns by use of equation 1, was calculated to be 39%  $\pm$  1.5%. Therefore  $AP = (\rho_V + \rho_{SL}) / .39$ . Figure 3 is a plot of this AP for waters of different turbidities.

Let subscript "1" indicate values for distilled water and subscript "2" indicate values from water sample #2 (a more turbid water). We can define  $AP_2 - AP_1$  as the "Laboratory Difference,  $D_2$ " between the laboratory apparent reflectances of samples #2 and #1 (distilled water).

$$D_2 = AP_2 - AP_1$$

$$D_2 = \frac{\rho_{V2} + \rho_{SL}}{\rho_{PL}} - \left( \frac{\rho_{V1} + \rho_{SL}}{\rho_{PL}} \right)$$

$$D_2 = \frac{\rho_{V2} - \rho_{V1}}{\rho_{PL}}$$

equation 4

REPRODUCIBILITY OF THE  
ORIGINAL PAGE IS POOR



From Figure 3 we see that for distilled water the average value of  $AP_1$

$$AP_1 = \frac{\rho_{v1} + \rho_{SL}}{\rho_{FL}} = 0.18\%$$

A usable value for  $\rho_{SL}$  is .020%. This leaves a value for  $\rho_{v1} = .18\%(.39) - .020\%$   
 $\rho_{v1} = .050\%$ .

From equation 4 if we have  $D_2$ ; we can calculate  $\rho_{v2}$  by

$$\begin{aligned}\rho_{v2} &= D_2 \rho_{FL} + \rho_{v1} \\ \rho_{v2} &= D_2 .39 + .05\%\end{aligned}$$

The value

$$D_2 = \frac{\rho_{v2} - \rho_{v1}}{\rho_{FL}}$$

is the important factor which will be further used to correlate between laboratory values and satellite values.

#### BOAT ANALYSIS

When the water being analyzed is out of doors as in Figure 5 we still have the direct radiance of the sun  $L'_S$ , which behaves analogously to the laboratory lamp in Figure 4. We also have  $L'_C$ , the average indirect radiance from the skylight. According to Lambert's Law the total irradiance effecting a horizontal surface due to this skylight is

$$H'_C = L'_C \pi.$$

The sun's direct contribution is  $H'_S = L'_S \psi \cos \theta$ . Let the total irradiance be  $H'_O$

$$\begin{aligned}H'_O &= H'_S + H'_C \\ H'_O &= L'_S \psi \cos \theta + L'_C \pi\end{aligned}$$

The diffuse signal from a field reflection panel,  $P$ , would be

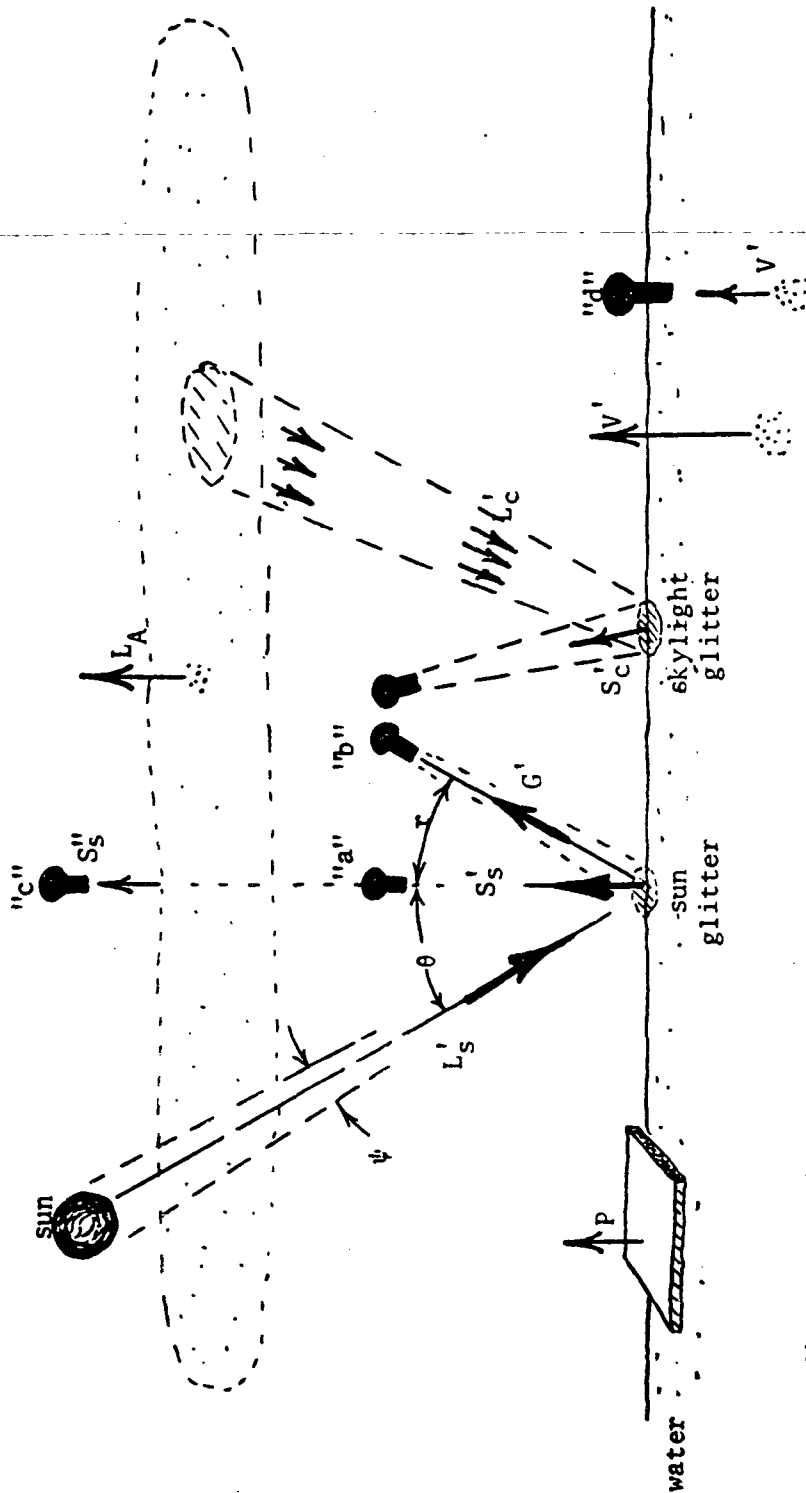
$$P = \frac{H'_O \rho_P}{\pi}$$

where  $\rho_P$  = the reflectance of this field panel.

Also following Lambert's Law for diffuse reflection,  $S'_S$ , the diffuse reflection caused by impurities on the water surface is:

$$S'_S = \frac{H'_O \rho_S}{\pi}$$

where  $\rho_S$  = the field diffuse reflection for foam, leaves, and other dirt



$L'_S$  = suns radiance reaching water

$L'_C$  = skylight radiance reaching water: skylight irradiance on panel is  $H'_C$ ;  $H'_C = \pi L'_C$

$S'_S, V'$ , are diffuse reflection from impurities on water surface and from material in water

$G', S'_C$ , are specular reflection of sunlight and skylight from water surface

Figure 5. Direct and Indirect Energy Relationships in the Field.

REPRODUCIBILITY OF THE  
ORIGINAL PAGE IS 100%

on the water surface. Also  $V'$ , the radiance from the water volume is

$$V' = \frac{H'_O \rho_V}{\pi}$$

The specular reflection of the sun from the water surface (sun glitter) is

$$G' = L'_S \epsilon = .020 L'_S$$

In a similar manner the specular reflection of the skylight from the water surface is  $S'_C$ .

$$S'_C = L'_C \epsilon = .020 L'_C$$

The total signal from the water is  $W'$ .

$$W' = V' + S'_S + S'_C$$

$$W' = \frac{\rho_V H'_O}{\pi} + \frac{\rho_S H'_O}{\pi} + .020 L'_C$$

$$W' = (\rho_V + \rho_S) \frac{H'_O}{\pi} + .020 L'_C$$

The signal from the field panel is

$$P' = \rho_P \frac{H'_C}{\pi}$$

If one were determining the volume reflectance of a particular lake in the field with the Bendix RPMI ground truth instrument this can most easily be done by pointing the RPMI sensor telescope down through the surface of the water as in position "d" in Figure 5. Assuming no significant bottom signal the sensor at "d" only reads the radiance from the water volume  $V'$ .

$$V' = \frac{\rho_V H'_O}{\pi}$$

$H'_O$  can be obtained directly by use of the RPMI or a reading can be taken on the panel,

$$P' = \rho_P \frac{H'_O}{\pi}$$

$$\frac{H'_O}{\pi} = \frac{P'}{\rho_P} \quad \text{and}$$

$$\rho_V = V' \frac{\rho_P}{P'}$$

Thus the  $\rho_V$  can also be obtained in the field for any water sample with the RPMI. However, due to variations in skylight and wave action in the field the laboratory determination of  $\rho_V$  is a magnitude more precise than field determinations.

# AIRBORNE ANALYSIS

When the signal from the water level such as  $S'_S$  in Figure 5 passes upward through the atmosphere it is attenuated by the atmospheric transmittance  $\tau$ ;  $S''_S = S'_S \tau$ . Also the atmospheric backscatter, LA, is added to the signal. Therefore, the total signal from the water as sensed at "c" in Figure 5, is

$$\begin{aligned} W'' &= (V' + S'_S + S'_C) \tau + LA \\ W'' &= \left( \frac{\rho_V H'_O}{\pi} + \frac{\rho_S H'_O}{\pi} + .020 L'_C \right) \tau + LA \\ W'' &= (\rho_V + \rho_S) \frac{H'_O}{\pi} \tau + .020 L'_C \tau + LA \end{aligned}$$

If we let subscripts 1 and 2 represent distilled or very clear water and a turbid lake (#2) respectively, then

$$\begin{aligned} W''_1 &= (\rho_{V1} + \rho_S) \frac{H'_O \tau}{\pi} + .020 L'_C \tau + LA \\ W''_2 &= (\rho_{V2} + \rho_S) \frac{H'_O \tau}{\pi} + .020 L'_C \tau + LA \end{aligned}$$

Also if we define the satellite residual  $R''_2$  to be the difference in signals which is caused only by the material in water #2, then

$$R''_2 = W''_2 - W''_1 = (\rho_{V2} - \rho_{V1}) \frac{H'_O \tau}{\pi}$$

Again assuming the volume reflectance of distilled water,  $\rho_{V1}$ , to be known,

$$\rho_{V2} = R''_2 \frac{\pi}{H'_O \tau} + \rho_{V1} \quad \text{equation 5}$$

With this  $\rho_{V2}$  one can enter the curve on Figure 3 and obtain turbidity. What is needed in the above situation is  $W''_1$ , a reading on a very clear lake. Then this reading can be subtracted from the reading from any other lake  $W''_i$ .

$$R''_i = W''_i - W''_1 \quad \text{and}$$

$$\rho_{Vi} = \left( R''_i \frac{\pi}{H'_O \tau} \right) + \rho_{V1}$$

If  $\frac{\pi}{H'_O \tau}$  is not known the answers are in relative terms only. If the  $\rho_{V2}$  of a turbid lake (sample #2) is known then from equation 5,

$$\frac{\pi}{H'_O \tau} = \frac{\rho_{V2}}{R''_2}$$

This  $\frac{\pi}{H'_O \tau}$  term can then be used to solve for the absolute volume reflectance of any lake.

The results in this paper are for relative values of  $\rho_{vi}$  only. The exact mathematical relationships were not fully understood at the time of the overflights in order to obtain the necessary simultaneous ground truth for sample #2.

### SATELLITE ANALYSIS

On the LANDSAT image assume we can locate a very clear lake, "#1", which approaches distilled water in purity. This lake must be deep enough so that no bottom is showing. Aerial observation should be made to assure that there are no bottom effects showing in this test lake.

Let  $W_1''$  equal the satellite raw reading on the clear lake. Let  $W_2''$  equal the raw reading on Lake #2, the lake in question. The raw readings for Band 4 and Band 5 are very high due to atmospheric effects and the differential water signals are perhaps 1% of these raw readings. The raw readings are not very meaningful. However, if we subtract  $W_1''$  from  $W_2''$  the residual is due only to the material in Lake #2.

$$R_2'' = W_2'' - W_1'' = (\rho_{v2} - \rho_{v1}) H_0' \frac{\tau}{\pi}$$

The four bands of LANDSAT cover as follows:

Band 4: 0.50 to 0.60 microns

Band 5: 0.60 to 0.70 microns

Band 6: 0.70 to 0.80 microns

Band 7: 0.80 to 1.10 microns

Let us plot the total signal from Bands 4, 5, 6, and 7, as centering on wavelengths 0.55, 0.65, 0.75, and 0.95 respectively. Figure 6 shows such a plot of the satellite residual,  $R_2''$ , for these four LANDSAT bands. Three types of waters; clear, tannin, and algal, are readily differentiated. Therefore, it is possible to separate lakes into these classes by LANDSAT signals alone. Also, within a particular class such as algal, one can categorize the lake as to how much algae is present. Figure 7 shows satellite residual signals of lakes which grade from clear to heavy algal.

The shape of the satellite residual curves of Figure 7 duplicate well the shape of the laboratory reflectance difference curves in Figure 8 for the same types of water. In Figure 7, the satellite residual

$$R_i'' = (\rho_{vi} - \rho_{vl}) H_0' \frac{\tau}{\pi}$$

In Figure 8, the laboratory reflectance differences are:

$$D_i = (\rho_{vi} - \rho_{vl}) \frac{1}{\rho_{PL}} = (\rho_{vi} - \rho_{vl}) \frac{1}{.39}$$

Therefore, the values on the two figures vary only by the factor:

$$\frac{R_i''}{D_i} = H_0' \frac{\tau}{\pi} \div \frac{1}{.39} = .39 H_0' \frac{\tau}{\pi}$$

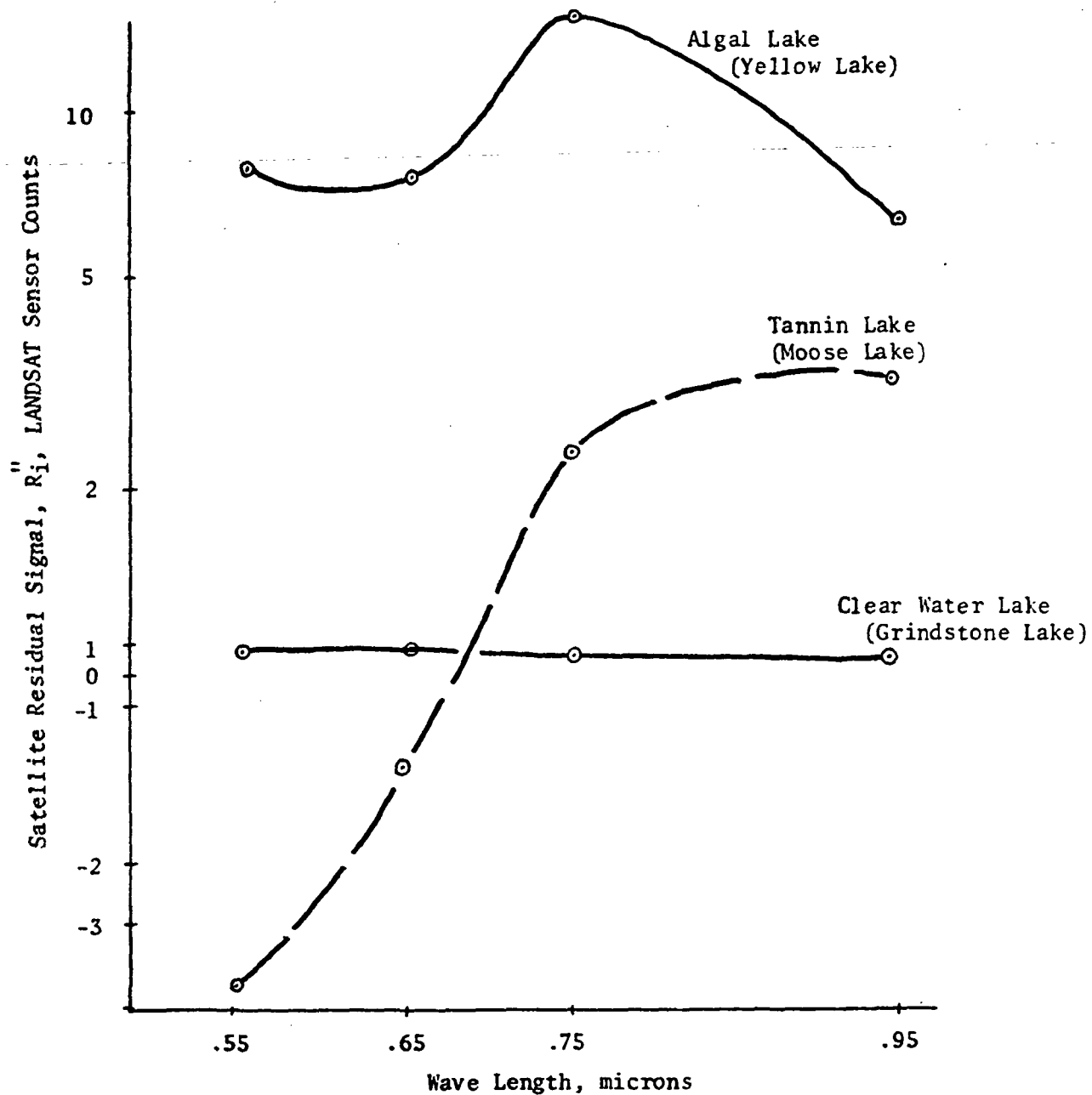


Figure 6. Satellite Residual Signal,  $R_i$ , for three water types.

$$R_i'' = W_i'' - W_1'' = (\rho_{vi} - \rho_{v1}) H_0' \frac{\tau}{\pi}$$

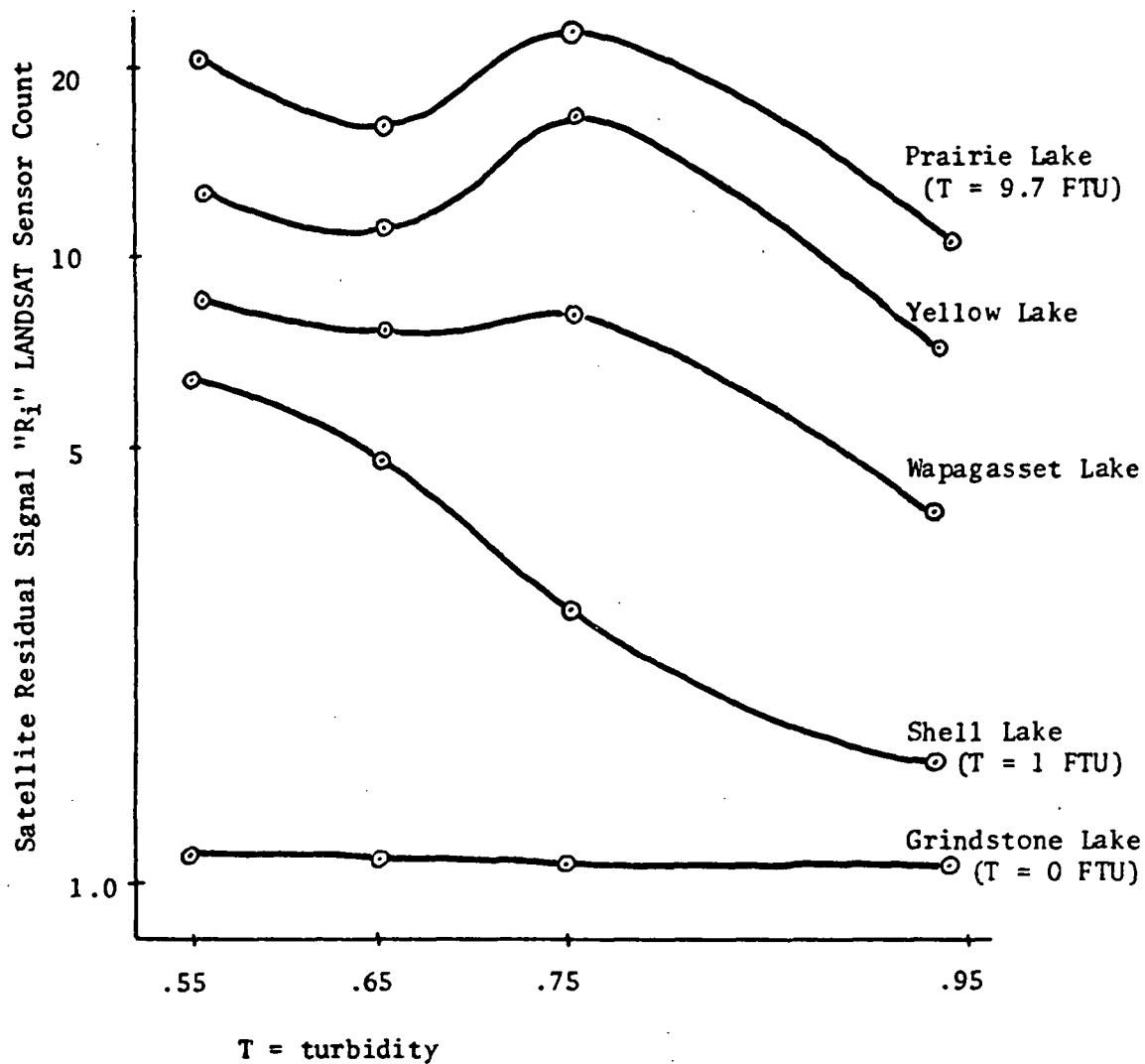


Figure 7. Satellite Residual Signal "R<sub>i</sub>" for clear-type water lakes with various amounts of algae present.

$$R_i = (\rho_{vi} - \rho_{vl}) H'_0 \frac{\tau}{\pi}$$

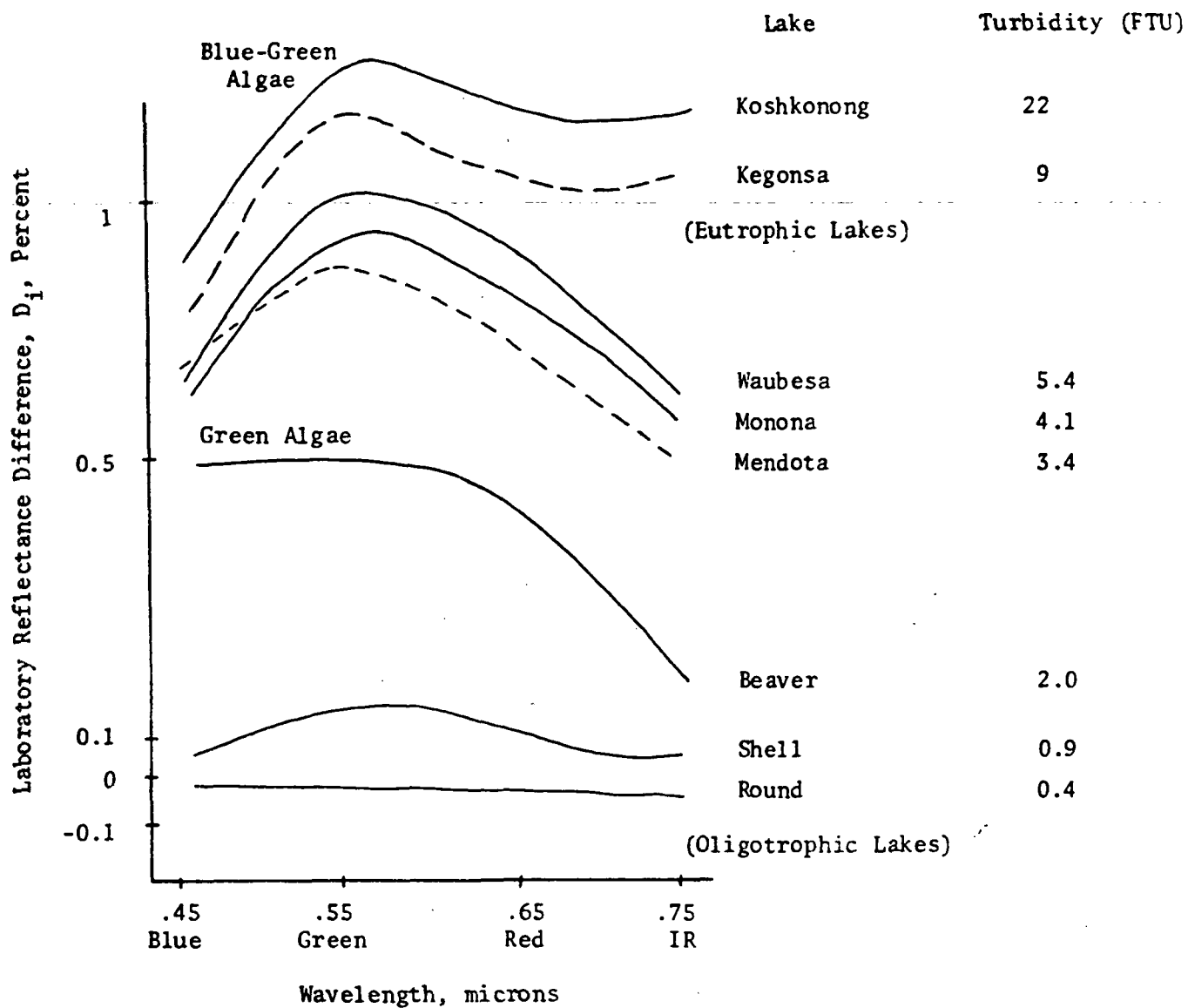


Figure 8. Laboratory Reflectance Difference Curves ( $D_i$ ) for clear-water type lakes with various amounts and types of algae present.

$$D_i = (\rho_{vi} - \rho_{vl}) \div \rho_{PL}$$



The gradation between heavy algal and clear water lakes are equally apparent in both Figures 7 and 8. Exact corresponding turbidities are also shown in Figure 8. Three approximate turbidities are shown in Figure 7. On Figure 8 one can also see that it is possible to tell the differences between types of algae. Blue-green and green algae types are indicated. Green algae are usually not the nuisance types but blue-green algae are, and are often associated with eutrophic lakes which can become low in dissolved oxygen.

Figure 9 shows that although the tannin type lakes have a different shaped characteristic curve, the more turbid tannin lakes have a higher signal and follow the same general pattern as with the algal lakes. Figure 9 also shows the relative ranges of the satellite and laboratory data.

#### OPTIMUM TIME OF YEAR FOR EUTROPHIC CLASSIFICATION

Figure 10 shows that in an individual lake the volume reflectance can change markedly from a characteristic clear water lake in early spring to a very algal lake in late summer and back to a clear water type lake in late fall. This is also indicated by Figure 1. The maximum algal and weed growth is in late August. This is also the time of minimum dissolved oxygen (see Figure 10) and also the time of maximum water temperature and when the nitrates become completely tied up in some lakes. From many indicators, late August is the optimum time for eutrophic classification of lakes.

#### BOTTOM PROBLEMS

The bottom effect problem is a difficult noise factor in satellite classification of lakes. Bottom signals can show in any of the lake types. The type of bottom (dark mud, light sand, or green weeds), also will give a different characteristic modification to signals from each of these water types. Also the depth to bottom effects the strength of the signal and also its spectral distribution.

It is anticipated that the bottom effect problem can be completely isolated by analyzing LANDSAT data from spring imagery when the lakes are clear and free of algae and the bottoms are very apparent. Where bottom signals are strong they are a characteristic signal and can be classified as another lake type. Figure 11 shows sand bottom and weed bottom effects on the satellite signals from a tannin type lake.

#### COLOR CATEGORIZED IMAGES PRODUCED BY THE BENDIX CORPORATION M-DAS EQUIPMENT

By training the Bendix M-DAS computer for each type of lake of interest the machine recognized all such types in the scene and displayed desired types as a color categorized image. It must be emphasized that good ground truth in the form of some water samples and aerial observations of the test lakes are essential for the training of the M-DAS equipment. The aerial observations are especially essential in locating the troublesome bottom effects which might show up on a training lake chosen without aerial observation.

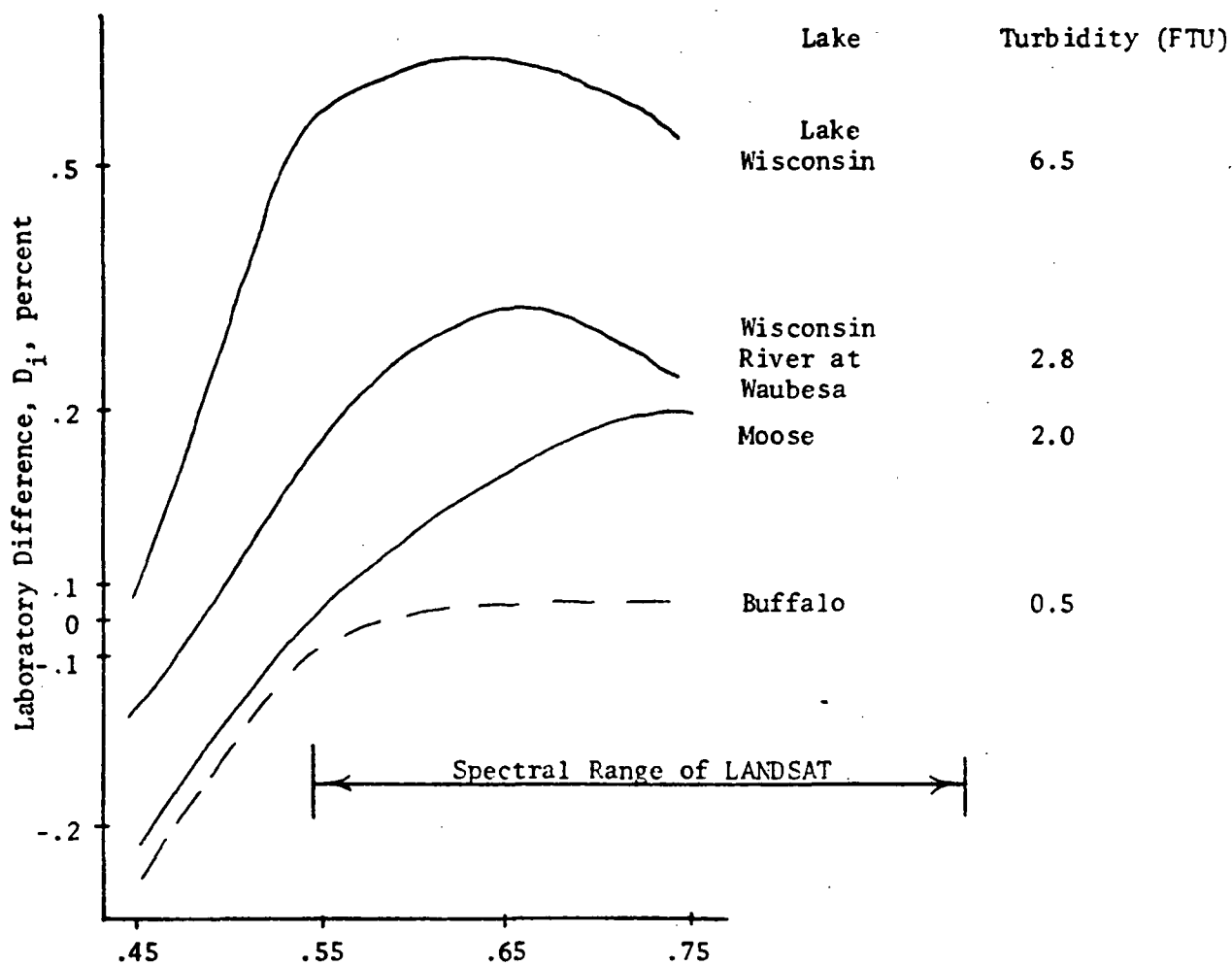
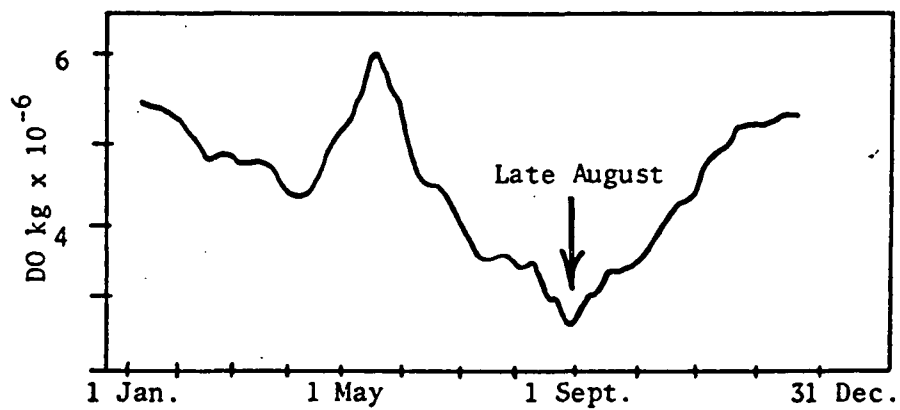
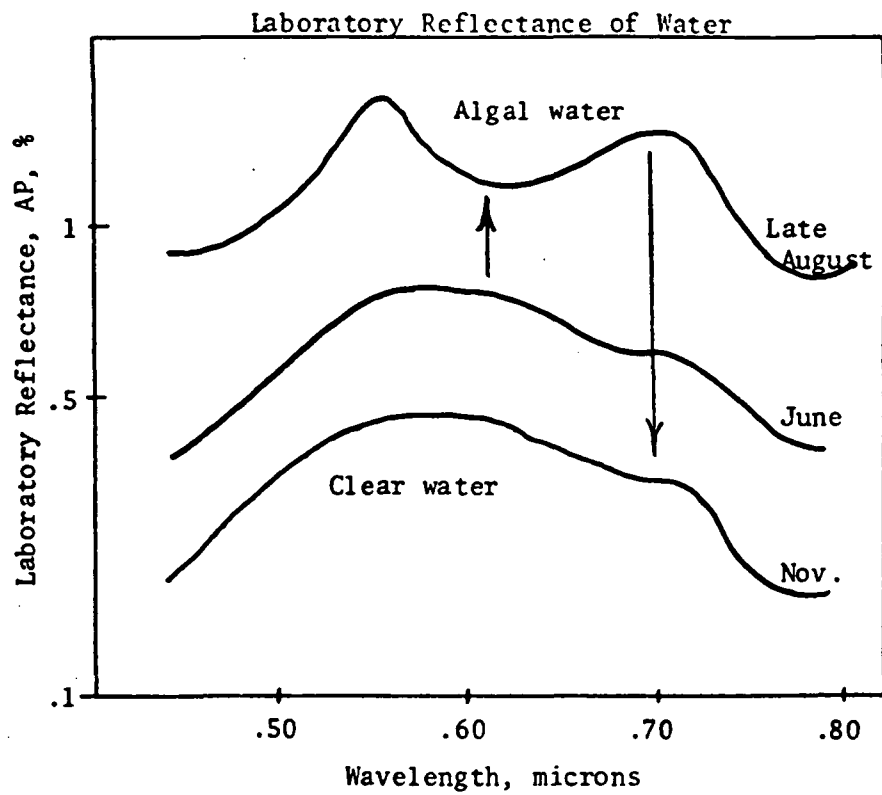


Figure 9. Laboratory Reflectance Difference Curves ( $D_i$ ) for tannin water lakes.



DO = Dissolved oxygen

Figure 10. Time of year effect on Laboratory Reflectance of Madison Area Lake. Maximum Reflectance occurs at the same time as minimum dissolved oxygen, which is late August.

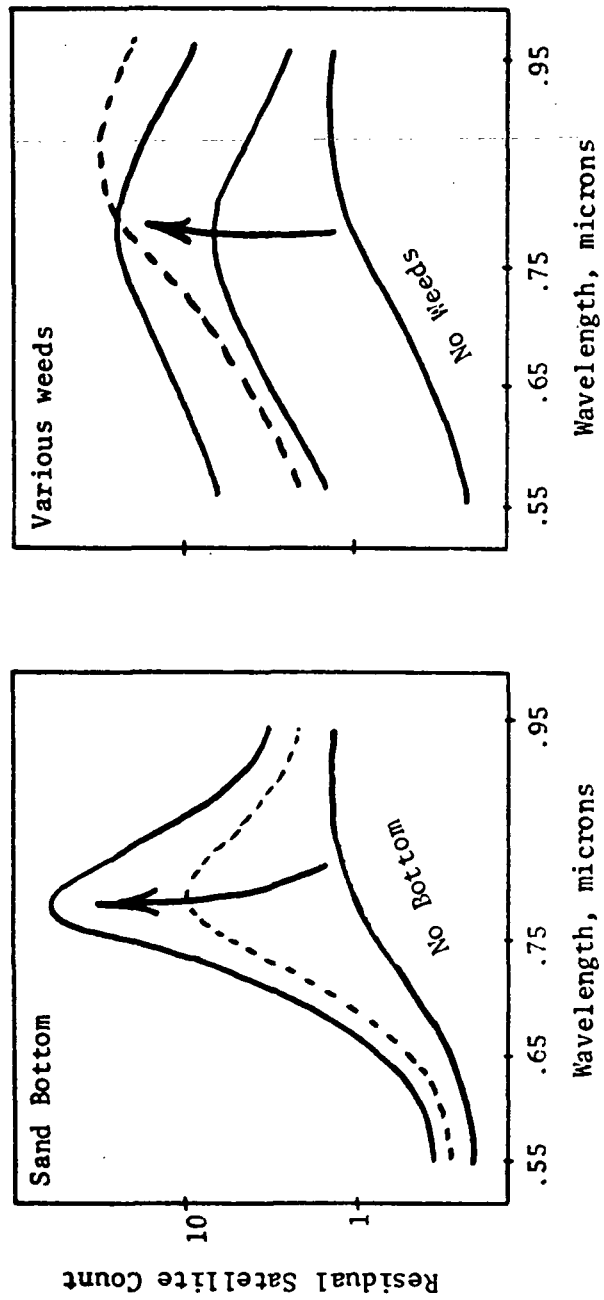


Figure 11. Effect of sand bottom and various kinds of weeds on satellite signal of a tannin-type lake.

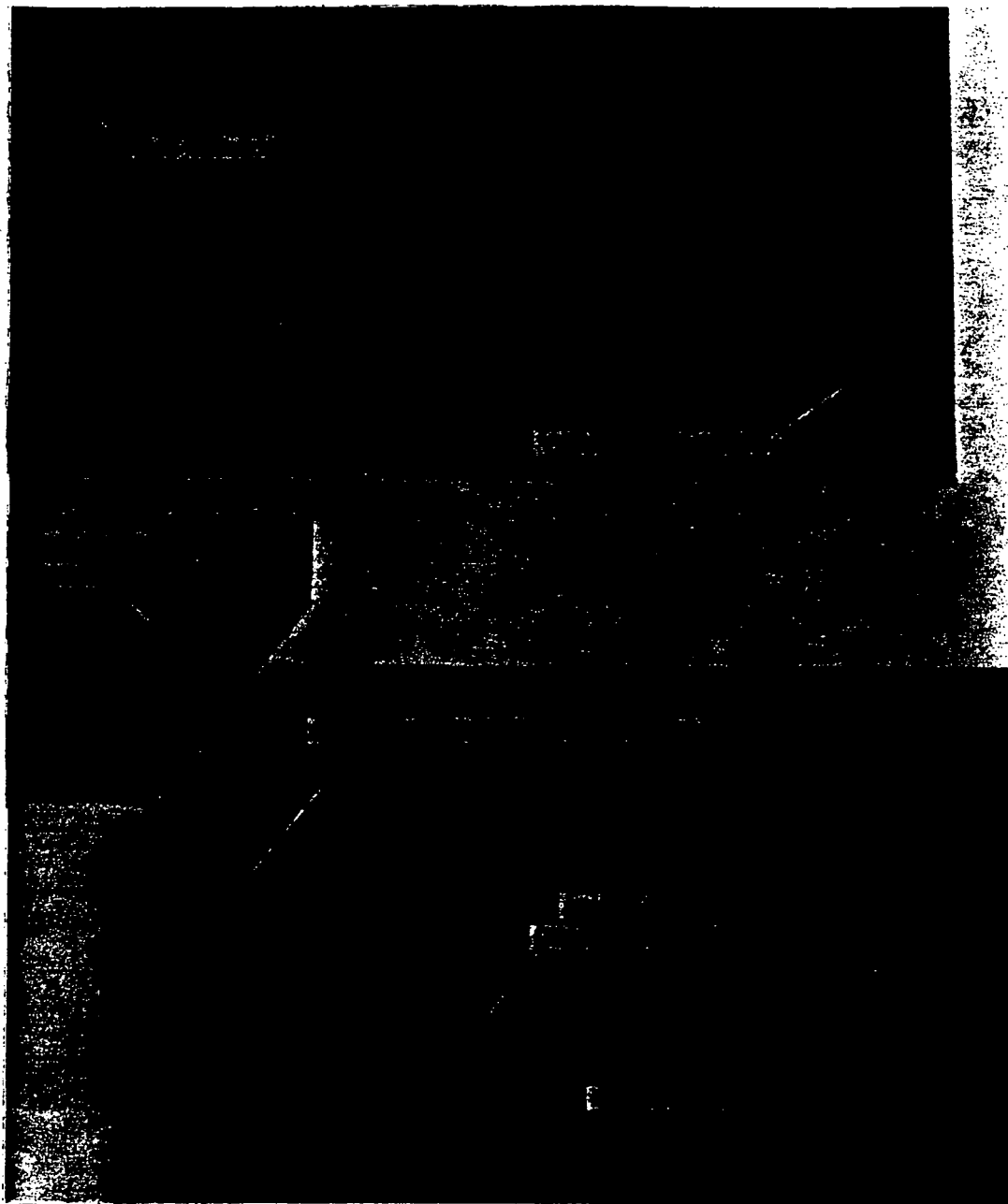


Figure 12 Initial Color Categorized Image Produced by Bendix Corp.  
Showing Lake Categorization. . (LANDSAT Scene 1756-16061  
of 18 August 1974)

Figure 12 shows the test color categorized image for lake categorization produced by the M-DAS equipment. The results look good and are being field checked in August, 1975. Further anticipated work includes combining spring imagery with summer imagery to completely solve the bottom effect problem.

#### ACKNOWLEDGEMENTS

The authors acknowledge the National Aeronautics and Space Administration for their support under Grant No. NGL 50-002-127, and NAS 5-20942 and those who helped administer these grants. The authors are also grateful to Francis Schraufnagle and other personnel from the Wisconsin Department of Natural Resources who helped especially in the field efforts. The authors also are grateful to those other persons from the University of Wisconsin and Bendix Aerospace Division who helped make this investigation possible.

#### REFERENCES

- (1) Piech, Kenneth R. and Walker, John E. "Aerial Color Analyses of Water Quality." Journal of the Surveying and Mapping Division - Proceedings of the American Society of Civil Engineers. November, 1971.
- (2) Rogers, Robert H.; Peacock, Keith; and Shah, Navinchandras J. "A Technique for Correcting ERTS Data for Solar and Atmospheric Effects." Paper 1-7 presented at the 3rd ERTS Symposium sponsored by NASA/GSFC, Washington D.C. December 10-14, 1973.
- (3) Psuty, Norbert P.; Allen, James R. "Trend-Surface Analysis of Ocean Outfall Plumes." Photogrammetric Engineering. June, 1975.
- (4) Gramms, Lorne C. "Reflectance and Transmittance Characteristics of Selected Green and Blue-Green Unialgae for Remote Sensing Application." PhD. Thesis, University of Wisconsin. 1971.
- (5) Scherz, James P., and Van Domelen, John F. "Lake Superior Water Quality near Duluth from Analysis of Aerial Photos and ERTS Imagery." Remote Sensing and Water Resources Management American Water Resources Association. June, 1973.